Prediction of the Liquid Vapor Pressure Using the Artificial Neural Network-Group Contribution Method

Tarjomannejad, Ali*[+]

Department of Chemical Engineering, University of Tabriz, Tabriz, I.R. IRAN

ABSTRACT: *In this paper, vapor pressure for pure compounds is estimated using the Artificial Neural Networks and a simple Group Contribution Method (ANN–GCM). For model comprehensiveness, materials were chosen from various families. Most of materials are from 12 families. Vapor pressure data of 100 compounds is used to train, validate and test the ANN-GCM model. Vapor pressure data were taken from literature for wide ranges of temperature (68.55-559.15 K). Based on results, the best structure for feed-forward back propagation neural network is Levenberg-Marquardt back propagation training algorithm, logsig transfer function for hidden layer and linear transfer function for output layer. The multiplayer network model consists of temperature, acentric factor, critical temperature, critical pressure and the structure of molecules as inputs, 10 neurons in the hidden layer and one neuron in the output layer corresponding to vapor pressure. The weights are optimized to minimize error between experimental and calculated data. Results show that optimum neural network architecture is able to predict vapor pressure data with an acceptable level. The trained network predicts the vapor pressure data with average relative deviation percent of 1.18%.*

KEY WORDS: *Artificial neural network, Group contribution method, Liquid vapor pressure, Equation of state.*

INTRODUCTION

Thermodynamic properties of pure fluids such as vapor pressure, density, heat capacity and thermal conductivity are very important in design of different chemical processes. Vapor pressure is one of the most important properties in chemical processes. The vapor pressure curve is unique for each substance, but the general shape of curve is similar for all of them [1]. For a limited number of substances vapor pressure has been reported in many points. The number of points is limited for most substances, so obtaining the equations for estimation and interpolation points is very important.

The vapor pressure can be obtained from equation of state. Two parameters equations of state such as *Peng-Robinson* [2], *Soave-Redlich-Kwong* [3] and *Patel Teja* [4] were widely used in predicting vapor pressure of compounds.

For predicting thermodynamic properties including vapor pressure, it can be used of Group Contribution Method (GCM). *Chein* [5] predicted the vapor pressure using of GCM. He predicted the vapor pressure by average absolute percentage deviation of 5%. *Avaullee et al.* [6] presented a group contribution method

* *To whom correspondence should be addressed.*
+ E-mail: ali_tarjoman@yahoo.com
1021-9986/15/4/97 15/$/3.50

for estimating the critical properties and acentric factors of paraffins, naphtenes and aromatics with emphasis on extrapolating to very heavy compounds. They predicted the properties with average deviation between 0.6 and 6.5%. *Marrero et al.* [7] predicted critical properties by using GCM. They showed the new method making significant improvements both in accuracy and applicability. *Coutsikos et al.* [8] presented a group-contribution model for the prediction of vapor pressures of organic solids. The obtained predictions by them are not very accurate. *Moller et al.* [9] presented a new group contribution method for the prediction of liquid vapor pressures for non-electrolyte organic compounds. They found the relative error of 5% in pressure. *Nannoolal et al.* [10] proposed a group contribution method for the estimation of the normal boiling point of nonelectrolyte organic compounds. *Ceriani et al.* [11] proposed a group contribution method for the estimation of vapor pressure and heat of vaporization of organic liquids. This method improved the prediction of normal boiling point.

The artificial neural networks can be a suitable alternative to model the different thermodynamic properties. An Artificial Neural Network (ANN) is an information processing method inspired from the human brain functioning rules [12]. ANN models are composed of computational points called neurons which are able to store experimental knowledge. ANNs are an especially efficient algorithm to approximate any function with a finite number of discontinuities by learning the relationships between the input and output vectors [13]. Thus, ANNs are appropriate techniques to model the nonlinear behavior of chemical properties.

Today, use of neural networks to predict thermodynamic properties such as vapor pressure is increasing. *Potukuchi et al.* [14] predicted vapor pressure of volatile inorganic compounds by using an artificial neural network. *Kuhne et al.* [15] investigated vapor pressure for hydrocarbons and halogenated hydrocarbons from chemical structure by using a Neural Network. *Potukuchi et al.* [14] predicted vapor pressure of volatile organic compounds including nitric acid, hydrochloric acid and ammonia. *Gandhidasan et al.* [16] predicted vapor pressures of aqueous desiccants for cooling applications by using an artificial neural network. Aqueous desiccants investigated by them included calcium chloride, lithium chloride, and lithium bromide. *Lazzus* [17,18] estimated solid vapor pressure for inorganic and inorganic compounds by a neural network. He investigated solid vapor pressure for 250 compounds. He also predicted vapor pressure and density of ionic liquids by using a neural network [19]. *Rohani et al.* [20] compared artificial neural network systems and SAFT equation to obtain vapor pressure and liquid density of pure alcohols.

In this paper, liquid vapor pressure is predicted by using a combined method that includes the Artificial Neural Networks and a simple Group Contribution Method (ANN–GCM). 100 substances have been investigated. To assess the accuracy of this model, calculated vapor pressure from ANN–GCM model and predicted by some EOSs, namely, Peng–Robinson, Soave–Redlich–Kwong and Patel Teja have been compared.

ARTIFICIAL NEURAL NETWORK

Artificial neural networks are used in a wide range of applications such as prediction of thermodynamic properties. Neural networks generally consist of a number of interconnected neurons that are organized in one or more layers. Usually, artificial neural networks are comprised of one input layer, one hidden layer and an output layer [21]. Output of each neuron is calculated by using transfer function (Eq. (1)).

$$y_j = F\left(S_j\right) \tag{1}$$

Where S_j, y_j and F are input of jth neuron before applying transfer function, output of jth neuron and transfer function. Input of each neuron is calculated from outputs of previous layers (Eq. (2)):

$$S_j = \sum_i w_{ij} y_i + b_j \tag{2}$$

Where w_{ij} and b_j are weights connecting ith neuron (from previous layer) and bias of jth neuron.

Common transfer functions are logarithmic function (logsig), hyperbolic tangent function (tansig) and linear

Table 1: Structural groups used in the proposed ANN+GCM method.

No.	Group	No.	Group
1	>C<	14	>N<
2	>CH-	15	-F
3	$-CH_2-$	16	-Cl
4	$-CH_3$	17	-I
5	$=CH_2$	18	-S-(Ring)
6	=CH-	19	$-CH_2-$(Ring)
7	≡CH	20	>CH–(Ring)
8	-O-	21	=CH–(Ring)
9	-OH	22	>C<(Ring)
10	>C=O	23	–O–(Ring)
11	=O	24	-NO
12	$-NH_2$	25	>N<(ring)
13	≡N	26	-H

function (purelin) that are defined in Eqs. (3) - (5), respectively:

$$y_j = \frac{1}{1+e^{-S_j}} \tag{3}$$

$$y_j = \frac{e^{S_j} - e^{-S_j}}{e^{S_j} + e^{-S_j}} \tag{4}$$

$$y_j = S_j \tag{5}$$

Number of inputs in the input layers depends on number of independent variables input and is defined by the nature of problem.

To evaluate the accuracy of proposed ANN model for prediction of liquid vapor pressure data at different temperatures, some statistical parameters, including Average Relative Deviation Percent (*ARD%*), the average deviation percent (*Bias%*), correlation coefficient (R^2) and the Root Mean Square Error (*RMS*) were utilized which are defined in Eqs. (6) - (9) [22,23]:

$$ARD\% = \frac{1}{N}\sum_{i=1}^{N} 100 \times \left| \frac{P_i^{exp} - P_i^{cal}}{P_i^{exp}} \right| \tag{6}$$

$$Bias\% = \frac{1}{N}\sum_{i=1}^{N} 100 \times \left(\frac{P_i^{exp} - P_i^{cal}}{P_i^{exp}} \right) \tag{7}$$

$$RMS = \sqrt{\frac{1}{N}\sum_{i=1}^{N}\left(P_i^{exp} - P_i^{cal}\right)^2} \tag{8}$$

$$R^2 = \frac{\sum_{i=1}^{N}\left(P_i^{exp} - \bar{P}\right)^2 - \sum_{i=1}^{N}\left(P_i^{exp} - P_i^{cal}\right)^2}{\sum_{i=1}^{N}\left(P_i^{exp} - \bar{P}\right)^2} \tag{9}$$

Where N is the number of liquid vapor pressure data points; P_i^{exp} is the ith experimental vapor pressure; P_i^{cal} is the predicted vapor pressure with ANN model and $\bar{P}$ is the average value of experimental vapor pressure data.

100 substances including 2044 points are investigated. Data are extracted from various articles [24-72]. These data were taken from paper that the experimental error reported less than ±1%. For train and testing the ANN model, 70% of the data are used to train the neural network and 20% for validating and 10% for testing. In this paper, liquid vapor pressure is estimated as a function of critical temperature, critical pressure acentric factor and temperature. [73-75]

In addition to these properties, the structure of molecules is considered as variables [6]. Table 1 shows 26 groups used as entrance variables. When the group does not appear in the substance, the value associated with the structural group is defined as 0. Some examples of the structure of molecules are shown in Table 2.

The chosen neural network is Feed-forward back propagation with Levenberg-marquardt back propagation training function. In this paper, one hidden layer is selected. To choose the best transfer functions for hidden and output layers different combinations of transfer

Table 2: Some examples of the structure of molecules.

Component	Formula	structural group				
R-134a	$C_2H_2F_4$	>C<	$-CH_2-$	-F		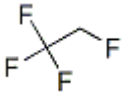
		1	1	4		
Ethyl butanoate	$C_6H_{12}O_2$	$-CH_3$	$-CH_2-$	-O-	>C=O	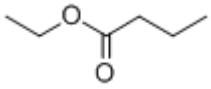
		2	3	1	1	
Trifluoroiodomethane	CF_3I	>C<	-F	-I		
		1	3	1		
Naphthalene	$C_{10}H_8$	=CH-(Ring)		>C< (Ring)		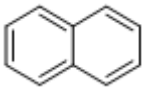
		8		2		

Table 3: The values of ARD% of different transfer functions with the optimal number of neurons in each case.

Transfer function		No. of neuron		ARD%
Logsig	Purelin	11	Train	1.4381
			Test	1.5853
Logsig	Tansig	12	Train	1.7574
			Test	1.9366
Logsig	Logsig	13	Train	3.0382
			Test	4.3307
Tansig	Purelin	10	Train	1.1743
			Test	1.2138
Tansig	Tansig	12	Train	1.6049
			Test	1.8401
Tansig	Logsig	10	Train	2.6401
			Test	3.1277

functions have been tested. Since no information about the optimal number of neurons has been reported for the calculation of liquid vapor pressure of substances, trial and error is the best way to determination the optimal number of neurons. The optimal number of neurons in the hidden layer was determined based on the minimum *ARD%*.

RESULTS AND DISCUSSION

Table 3 shows *ARD%* of different transfer functions with the optimal neurons number in each case. According to Table 3, neural network with tansig-purelin transfer functions with 10 neurons in hidden layer has the least *ARD%*. Fig. 1 shows the values of *ARD%* in contrast with different neurons number in hidden layer with tansig-purelin transfer function. Table 4 shows the *ARD%*, RD_{max}, *Bias%*, R^2 and *RMS* for all data sets using the proposed neural network.

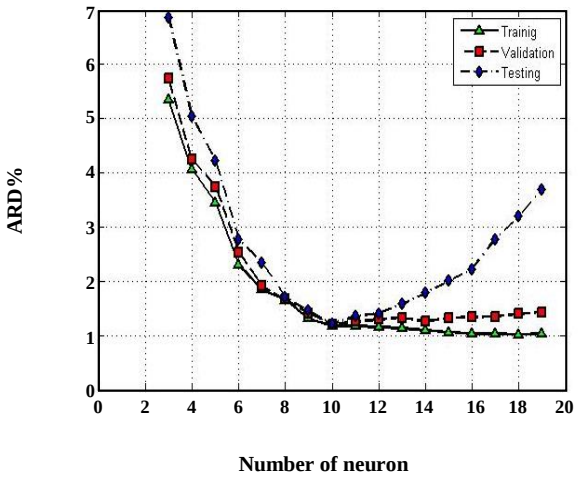

Fig. 1: Average absolute deviation (ARD%) as a function of the number of neurons in the hidden layer

Table 4: Statistical parameters for data sets.

	ARD%	RD_{max}	Bias%	RMS	R^2
Training set	1.1743	14.0604	-0.0414	0.0210	0.999994
Validation set	1.1983	17.1748	-0.2848	0.0217	0.999997
Testing set	1.2138	10.5827	-0.0726	0.0214	0.999997
Total set	1.1830	17.1748	-0.0932	0.0212	0.999995

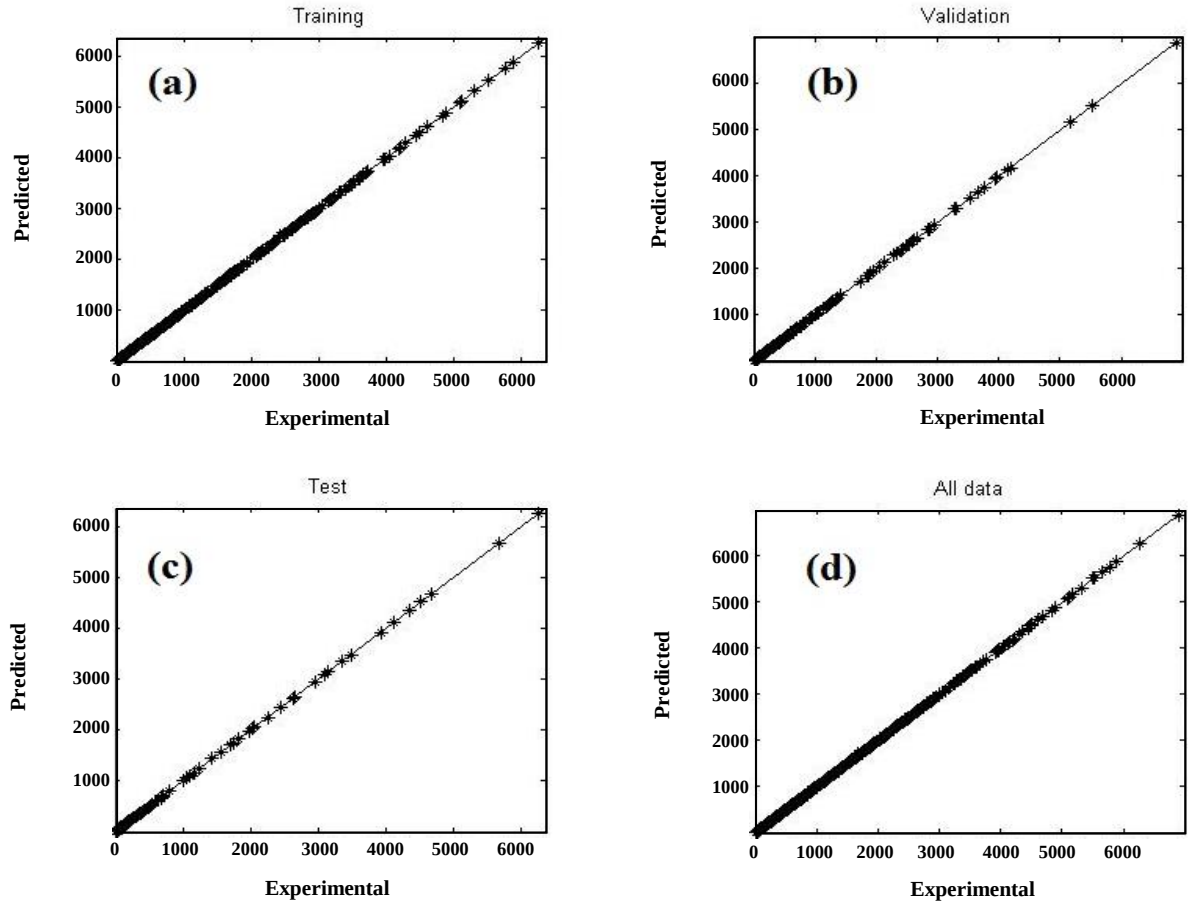

Fig. 2: Comparison between predicted and experimental data for training (a), validation (b), test (c) and total data (d) sets

The results show that the artificial neural network can be accurately trained and that can estimate the liquid vapor pressure with acceptable accuracy. In this estimating, the root mean square error is 0.021, 0.022 and 0.21 respectively for the training, validation and test data.

Comparisons between experimental and calculated values for all data sets are shown in Fig. 2. The optimum weights and biases for the neural network are shown in Table 5. The weights and biases in Table 5 are able to recalculate the obtained results in this paper.

To assess the accuracy of the this model in prediction of liquid vapor pressure, the ARD% values between experimental and calculated vapor pressure from ANN–GCM model and predicted by some other methods, namely, Peng–Robinson, Soave–Redlich–Kwong and Patel Teja have been compared. The three equations of state were used for prediction of phase behavior of all substances.

The results for each substance are illustrated in Table 6. Four last columns in the table show these average relative

Table 5: The weight and bias values of the optimal architecture.

Neuron	**1**	**2**	**3**	**4**	**5**	**6**	**7**	**8**	**9**	**10**
T	3.1790	0.0389	0.0657	3.0672	2.5814	2.9727	0.0121	3.5517	-2.6035	-2.3839
T_c	-1.4526	-1.5128	1.8472	-0.9421	-3.0187	-4.4137	0.0023	1.2904	3.0202	3.0399
P_c	0.0873	0.7597	-1.1891	0.7637	1.1003	0.8235	-0.0218	-2.3599	-1.0282	-1.1226
ω	-1.5685	-0.3218	0.4540	-1.3973	-0.6499	-0.1957	-0.0094	3.1082	1.3910	0.5295
>C<	-0.5018	0.1512	-0.1129	-0.5765	-0.0056	-0.2755	-0.0239	-1.3963	1.3994	-0.0182
>CH-	-0.2717	0.3157	-0.3519	-0.3414	0.0418	-0.0058	-0.0121	-0.2721	-0.0772	-0.0636
-CH2-	-0.8591	0.2035	-0.1595	-0.6318	-0.5141	-0.3609	-0.0032	0.7454	1.9981	0.5384
-CH3	-0.0949	-1.0044	0.7774	-0.7547	-0.0578	0.4666	0.0451	1.3914	-1.4271	0.1194
=CH2	0.9999	0.1803	0.1364	0.3652	0.1123	-0.3379	-0.5894	-2.1147	0.8298	-0.1378
=CH-	-0.3575	-0.3952	0.0730	0.1725	-0.2121	-0.2495	0.0069	-0.6650	-0.2586	0.23066
≡CH	0.2799	0.0328	-0.4086	0.5553	-0.1781	-0.2455	0.5861	-0.4507	0.02183	0.1840
-O-	-0.8481	-0.6060	1.4125	-0.7676	-0.1553	-0.2706	-0.0029	2.1250	0.6684	0.1945
-OH	0.1854	-0.0402	-0.0862	-0.2753	0.0306	0.51007	0.0146	-0.3961	-1.5567	-0.0042
>C=O	0.1088	-0.1617	0.0668	-0.0200	-0.0187	0.1809	0.0098	0.5123	0.2643	0.0119
=O	-1.5366	-0.1316	-0.1018	-0.4519	0.0456	-0.0031	0.0331	-0.7124	1.1358	-0.0333
–NH2	0.4097	-0.5378	0.4475	-0.4758	-0.229	0.3351	0.0380	-0.7249	0.5088	0.2408
≡N	1.3794	-0.4204	-1.1464	1.4089	-0.2805	0.3370	0.7334	-0.6440	0.2434	0.0144
-F	1.0016	0.0841	-0.2830	0.8677	-0.1121	0.4453	0.0228	0.0033	-0.1356	0.2160
-Cl	0.6871	0.4427	-0.8256	0.6723	-0.2666	-0.0346	0.4349	-1.7958	-1.6765	0.3438
-I	0.6862	0.2578	-0.3742	0.7180	-0.0041	0.0302	0.0589	1.1860	-1.5286	-0.0889
-S-(ring)	1.5980	-0.0030	0.6069	0.2394	0.0392	0.5324	-0.0307	0.0256	-0.1789	-0.2143
–CH2–(ring)	0.1571	-0.1370	0.0527	-0.0681	-0.0284	-0.1840	0.0150	1.2048	-0.2807	0.0482
>CH–(ring)	-2.9784	-0.0606	0.2764	-3.2277	-0.1731	-0.6134	-0.0345	0.5368	0.5306	0.2110
=CH–(ring)	-0.0121	-0.5558	0.3832	-0.2617	-0.0222	0.0910	0.0229	0.8595	-0.5632	0.0335
>C<(ring)	-0.9727	0.2892	0.0741	-1.1641	-0.0856	-0.2715	-0.0208	-0.3217	-0.2257	0.1309
–O–(ring)	0.6645	0.2271	-0.2448	0.5166	0.4389	0.2720	-0.0669	0.0272	-0.4474	-0.4259
-NO	0.9408	0.4756	-0.8520	1.5007	0.5499	0.5373	0.0876	0.5385	-0.3447	-0.4109
>N<(ring)	-1.0456	0.2473	-0.6771	0.3668	0.1098	0.4167	0.2709	0.3552	-1.6013	-0.0364
-H	1.4655	0.3270	-0.6212	0.5894	-0.3884	0.4989	0.1489	0.3211	-0.7827	0.2096
>N<	0.8210	0.1107	-0.0424	1.0511	0.3609	0.2161	-0.0248	-0.3774	-0.1669	-0.3767
Bias	-1.4948	-2.0845	-1.1197	-2.5030	-1.8673	-1.1423	0.0521	0.9029	1.0902	1.6648
Output layer weights	-2.7942	-2.3020	-0.9860	3.4034	2.7796	6.9701	-1.2553	0.0378	2.9561	2.7800
Bias										1.1119

Table 6: More detailed results about the correlated values.

	Name	Formula	T (K)	P (kPa)	ARD%			
					PR	SRK	PT	ANN
1	Methane	CH_4	96.48-122.03	23.52-220.08	0.53	4.39	28.91	0.67
2	Ethane	C_2H_6	165-300	30.67-4353.5	0.48	1.34	12.90	0.48
3	n-Butane	C_4H_{10}	280-424	133-3716.9	0.44	4.20	1.11	0.41
4	Isobutene	C_4H_8	310-407	488.4-3584.3	0.27	5.14	0.75	0.03
5	n-Pentane	C_5H_{12}	297.04-322.04	66.53-153.75	0.48	5.34	1.48	0.45
6	n-Hexane	C_6H_{14}	294.26-372	17-237.74	0.76	1.45	1.41	0.89
7	n-Octane	C_8H_{18}	338.71-399.82	12.57-103.63	4.20	2.71	12.43	1.35
8	n-Decane	$C_{10}H_{22}$	371.21-392.79	8.82-19.92	1.28	1.88	21.23	1.77
9	Hexadecane	$C_{16}H_{34}$	495.45-559.15	20.00-101.33	2.12	2.14	26.99	2.10
10	Acetylene	C_2H_2	193.15-213.15	133.48-354.18	0.58	9.5	0.59	0.02
11	Butadiene	C_4H_6	233.75-343.85	20.45-939.2	1.53	6.70	1.93	1.31
12	Butylene	C_4H_8	255.37-291.48	34.76-140.52	3.70	7.64	24.51	1.11
13	1-Hexene	C_6H_{12}	389.32-499.76	456-5.3003	2.31	2.26	2.45	0.36
14	Benzene	C_6H_6	283.25-373.45	5.74-182.65	4.50	1.75	8.20	1.03
15	Cyclohexane	C_6H_{12}	283.85-551.23	6.97-3951.41	3.41	1.05	7.74	0.77
16	Toluene	C_7H_8	324.06-402.21	12.136-166.04	3.66	1.28	3.18	0.86
17	m-Xylene	C_8H_{10}	333.15-399.82	6.09-71,78	2.67	2.53	29.51	2.52
18	p-Xylene	C_8H_{10}	333.15-399.82	6.58-73.57	2.28	4.61	1.58	1.06
19	Naphthalene	$C_{10}H_8$	358.85-491.79	1.29-102.95	2.46	2.92	1.64	2.38
20	n-Butylbenzene	$C_{10}H_{14}$	353.45-418.04	2.82-37.03	4.38	4.66	11.49	2.75
21	5-Ter-butyl-m-xylene	$C_{12}H_{18}$	383.06-442.9	4.4-37.78	6.11	7.53	8.58	2.69
22	n-Hexylbenzene	$C_{12}H_{18}$	422.76-462.97	11.83-40.69	1.83	1.84	17.07	1.76
23	Ethylbenzene	C_8H_{10}	366.48-466.48	21.25-311.87	1.91	3.20	3.25	1.15
24	Acetic acid	$C_2H_4O_2$	349.82-422.04	24.24-239.87	3.16	4.34	11.21	1.40
25	Acetic acid butyl ester	$C_6H_{12}O_2$	319.45-397.75	9.17-147.39	6.27	7.65	2.98	2.94
26	Oleic acid	$C_{18}H_{34}O_2$	513.10-524.70	2.66-9.33	10.49	7.09	7.17	4.29
27	Acetone	C_3H_6O	268.95-338.95	7.44-136.63	2.23	1.65	1.18	0.94
28	2-Butanone	C_4H_8O	305.22-388.55	17.99-282.20	1.13	2.03	1.67	1.23
29	2-Hexanone	$C_6H_{12}O$	294.11-399.66	1.80-100.32	8.43	11.56	3.71	2.26
30	n-Hexanal	$C_6H_{12}O$	343.15-363.15	15.10-32.14	5.39	7.97	7.45	2.99
31	Diethyl ether	$C_4H_{10}O$	301-396	79.28-1080.15	1.49	1.60	2.91	1.30
32	Ethyl butanoate	$C_6H_{12}O_2$	305.22-427.44	2.70-245.03	3.13	4.85	11.27	2.60

Table 6: More detailed results about the correlated values. (Continued)

33	Tetrahydrofuran	C_4H_8O	288.15-339.05	15.20-101.33	3.74	2.17	6.57	1.53
34	Ethyl acetate	$C_4H_8O_2$	350.19-373.15	3.14-10.72	20.16	24.13	31.67	4.47
35	Acetaldehyde	C2H4O	260.93-324.82	24.59-320.16	10.82	5.86	12.96	0.95
36	Acrolein	C3H4O	299.82-372.03	49.99-486.74	13.63	14.54	13.33	3.85
37	Chloroform	$CHCl_3$	293.15-334.35	21.09-101.33	2.11	5.28	11.83	1.98
38	HFC-227ea	C_3HF_7	249.03-373.80	54.05-2859.22	0.68	0.85	3.91	0.46
39	HFC-236fa	$C_3H_2F_6$	239.024-397.97	20.71-3174.16	23.43	23.37	20.74	0.63
40	HFC-245fa	C3H3F5	261.47-424.32	30.38-3479.18	0.67	0.36	3.84	0.32
41	HFC-32	CH_2F_2	233.15-351.15	177-5767.9	0.60	1.36	1.07	0.10
42	HFC-161	C_2H_5F	253.15-323.15	216.2-17003.9	1.20	1.43	5.36	0.46
43	R-12	CCl_2F_2	203.15-383.15	12.3-3978.5	0.94	0.87	7.32	0.90
44	R-22	$CHClF_2$	203.15-368.15	20.5-4883.5	1.63	1.17	4.62	0.92
45	R-134a	$C_2H_2F_4$	233.15-373.15	51.8-3973.2	0.31	1.10	0.95	0.25
46	R123	$C_2HCl_2F_3$	271.55-308.06	29.9-129.9	15.19	13.21	7.10	1.08
47	R141b	$C_2H_3Cl_2F$	270.92-312.31	25.41-129.11	1.55	1.29	7.78	0.07
48	Trifluoroiodomethane	CF_3I	243.15-325.15	71.7-982.6	0.89	0.75	8.52	0.05
49	Sulfolane	$C_4H_8O_2S$	421.89-516.333	1.95-39.34	1.51	5.43	7.10	1.00
50	Methanol	CH_4O	292.56-337.65	12.01-101.25	2.79	6.10	23.39	1.19
51	Ethanol	C_2H_6O	273.15-351.7	1.59-102.22	1.13	3.15	39.22	2.01
52	1,2-Ethanediol	$C_2H_6O_2$	389.12-495.44	4.70-201.40	3.32	3.99	29.23	2.02
53	2-Propanol	C_3H_8O	310.93-372.04	12.42-191.65	4.09	3.06	39.28	2.05
54	Isopropyl alcohol	C_3H_8O	305.372-372.04	9.69-191.61	3.34	2.33	39.59	1.32
55	1-Butanol	$C_4H_{10}O$	333.15-341.48	9.28-13.75	5.18	3.87	44.71	4.19
56	1-Hexanol	$C_6H_{14}O$	366.67-432.33	8.32-106.98	7.35	6.06	34.09	2.90
57	1-Heptanol	$C_7H_{16}O$	382.30-452.97	8.32-111.28	7.34	6.17	32.53	2.34
58	1-Octanol	$C_8H_{18}O$	397.32-465.29	8.35-93.54	6.63	5.39	34.35	1.12
59	1-Nonanol	$C_9H_{20}O$	422.04-516.48	12.99-205.88	2.90	2.66	25.95	2.64
60	1-Tetradecanol	$C_{14}H_{30}O$	479.42-519.183	8.32-29.35	1.65	1.34	47.05	1.31
61	1-Methylmorpholine	$C_5H_{11}NO$	273.18-353.08	6.9-332.76	99.80	99.82	99.74	1.83
62	2-Methoxyethanol	$C_3H_8O_2$	346.6-416.6	15-176.5	6.98	7.75	36.48	1.11
63	1-Methoxy-2-propanol	$C_4H_{10}O_2$	342.3-411.8	15-176.5	29.42	29.44	4.07	1.19
64	2-Methyl-1-propanol	$C_4H_{10}O$	351.2-392.2	30-150	3.68	3.26	27.67	2.30
65	Acetonitrile	C_2H_3N	293.14-379.13	9.42-205.90	3.26	5.46	9.21	0.92
66	Ethanolamine	C_2H_7NO	372.04-442.04	5.48-55.08	20.64	19.35	10.05	3.44
67	Aniline	C_6H_7N	355.37-372.04	2.83-6.47	7.16	14.37	5.36	4.34

Table 6: More detailed results about the correlated values. (Continued)

68	Pyridine	C_5H_5N	316.48-442.03	7.06-280.18	6.82	7.59	11.554	2.49
69	Ammonia	NH_3	223.15-387.15	40.9-6890.4	0.48	1.71	4.38	0.27
70	Carbon dioxide	CO_2	235.78-296.88	1113.5-6255.61	1.87	1.03	4.70	0.02
71	Nitrogen	N_2	68.55-91.89	28.38-453.81	4.57	3.33	21.88	1.79
72	Water	H_2O	281.15-373.15	1.1-101.3	12.81	22.36	8.83	1.54
73	Oxygen	O_2	92.59-99.82	126.59-250	2.01	0.55	22.67	0.52
74	n-Butylcyclopentane	C_9H_{18}	343.15-402.26	5.53-47.51	2.45	1.59	8.72	1.90
75	Cyclopentane	C_5H_{10}	273.3-343.21	14.34-191.64	2.16	1.39	10.35	1.29
76	Methylcyclohexane	C_7H_{14}	284.62-392.24	3.13-163.7	2.57	1.48	6.25	1.84
77	Ethylcyclohexane	C_8H_{16}	324.54-427.18	6.38-176.39	5.99	3.18	3.04	1.42
78	n-Propylcyclohexane	C_9H_{18}	334.63-452.22	3.88-171.82	10.73	7.33	6.01	2.42
79	Isopropylcyclohexane	C_9H_{18}	324.63-452.27	2.63-180.57	1.79	1.52	3.09	1.42
80	n-Butylcyclohexane	$C_{10}H_{20}$	352.04-467.15	3.47-137.73	13.11	9.82	9.25	2.83
81	n-Hexylcyclohexane	$C_{12}H_{24}$	422.22-467.26	12.2-47.38	2.03	1.05	21.35	0.94
82	n-Heptylcyclohexane	$C_{13}H_{26}$	402.21-467.21	3.01-28.43	4.23	2.00	33.83	0.71
83	n-Octylcyclohexane	$C_{14}H_{28}$	432.13-467.18	5.47-17.01	1.29	1.63	34.09	1.17
84	Diethyl phthalate	$C_{12}H_{14}O_4$	479.25-520.32	8.32-29.35	2.85	2.66	54.42	1.37
85	Cyclohexylbenzene	$C_{12}H_{16}$	383.01-462.66	1.78-29.7	2.48	2.54	10.54	1.95
86	n-Octylbenzene	$C_{14}H_{22}$	432.94-462.87	5.14-14.26	3.60	2.99	35.33	2.33
87	di-Butylsulfide	$C_8H_{18}S$	325.09-422.78	1.50-61.29	53.05	55.07	43.79	4.79
88	di-Sec-butylsulfide	$C_8H_{18}S$	342.02-422.17	3.43-63.13	70.92	65.92	70.92	3.14
89	1,2–Bis(dimethylamino)ethane	$C_6H_{16}N_2$	294.75-364.97	1.77-40.04	6.22	16.08	1.56	1.26
90	Ethyl methanoate	$C_3H_6O_2$	300-326.52	35.53-98.75	1.12	1.33	1.99	0.78
91	Ethyl butanoate	$C_6H_{12}O_2$	341.38-393.55	16.16-99.4	1.09	1.06	8.65	1.08
92	Propyl methanoate	$C_4H_8O_2$	309.09-352.95	18.52-99.07	2.16	1.24	1.85	1.08
93	Propyl ethanoate	$C_5H_{10}O_2$	343.59-371.75	35.63-93.9	0.39	1.54	6.44	1.21
94	Cumene	C_9H_{12}	346.69-392.87	15.14-39.87	2.39	0.97	3.38	0.56
95	3-Pentanone	$C_5H_{10}O$	347.05-364.75	40.01-73.35	2.04	1.45	4.75	1.35
96	3-Methylbutan-2-one	$C_5H_{10}O$	328.88-362.36	26.58-86.52	2.82	3.24	0.74	0.72
97	2-Hexanone	$C_6H_{12}O$	307.76-385.47	2.46-64.38	2.61	2.02	10.80	1.72
98	3-Hexanone	$C_6H_{12}O$	361.63-382.57	33.05-66.53	0.70	1.22	6.76	0.66
99	2-Heptanone	$C_7H_{14}O$	345.14-424.13	6.43-101.11	1.59	0.53	12.08	0.41
100	5-Nonanone	$C_9H_{18}O$	393.765-414.02	12.45-25.76	0.74	1.19	22.05	0.39
	Overall				5.55	5.68	12.91	1.18

Table 7: Compare the results from ANN-GCM with EOSs for each group.

Family	ARD%			
	PR	SRK	PT	ANN
Hydrocarbon	1.436	4.206	10.514	0.842
Aromatic	3.847	3.067	14.283	1.676
ester	1.190	1.292	4.732	1.037
ether	7.130	8.187	13.105	2.475
Aldehyde	9.946	9.456	11.246	2.596
Amin	11.540	13.778	8.988	3.423
Alcohol	12.994	12.937	37.834	1.944
Refrigeration	3.418	3.065	6.048	0.545
Hydrofluorocarbon	5.316	5.474	6.984	0.394
ketone	2.476	2.765	7.082	1.075
Halogen	2.116	5.28	11.833	1.984
Acid	6.641	6.36	7.120	2.876

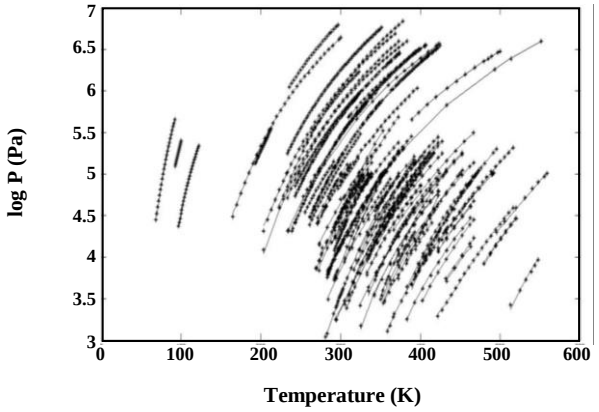

Fig. 3: Comparison between ANN predicted (-) and experimental data.

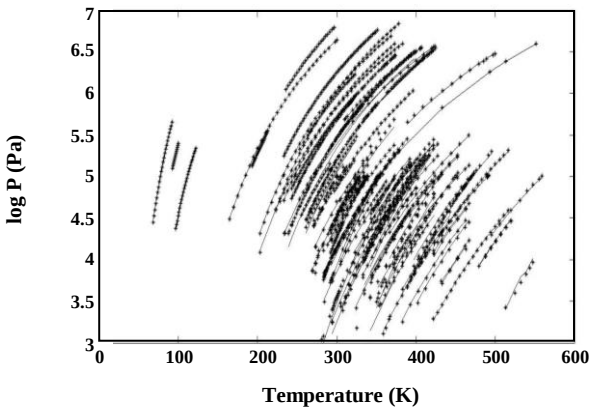

Fig. 4: Comparison between Peng-Robinson predicted (-) and experimental data.

deviation percents for various models. The predictions of ANN–GCM model are better than investigated EOSs. As observed in this table, for EOSs the average relative deviation percents have a wide range for substances but for neural network model the average relative deviation percents for these substances are within the same ranges. Comparisons between experimental and calculated values for ANN model and EOSs are shown in Figs. 3 to 6. The results from ANN-GCM with EOSs for each group are compared and shown in Table 7. For all of group, AAN model can predict the vapor pressure data better than EOSs.

CONCLUSIONS

In this work, artificial neural network model is developed to estimate the liquid vapor pressure of pure substances. From 2044 existence points, 70% of them have applied for training, 20% for validating and 10% for testing. Based on obtained results, the best structure for neural network is Feed-forward back propagation network, Levenberg-marquardt back propagation training function, tangsig transfer function for hidden layer and purelin transfer function for output layer. Optimal number of neuron in hidden layer is 10 neurons. The weights are optimized to minimize the derivation between the calculated and experimental liquid vapor pressure data. The relative average error in estimating the vapor-liquid equilibrium was found to be quite low. The obtained results show that the optimum neural network architecture was able to predict vapor pressure data with an acceptable level of accuracy of *ARD %* of 1.183, R^2 of 0.999995, *Bias%* of -0.093 and RMS of 0.021.

Table A.1: Number of structural group for Ethyl butanoate.

No.	Group		No.	Group	
1	>C<	0	14	>N<	0
2	>CH-	0	15	-F	0
3	$-CH_2-$	2	16	-Cl	0
4	$-CH_3$	3	17	-I	0
5	$=CH_2$	0	18	-S-(Ring)	0
6	=CH-	0	19	$–CH_2–$(Ring)	0
7	≡CH	0	20	>CH–(Ring)	0
8	-O-	1	21	=CH–(Ring)	0
9	-OH	0	22	>C<(Ring)	0
10	>C=O	1	23	–O–(Ring)	0
11	=O	0	24	-NO	0
12	$–NH_2$	0	25	>N<(ring)	0
13	≡N	0	26	-H	0

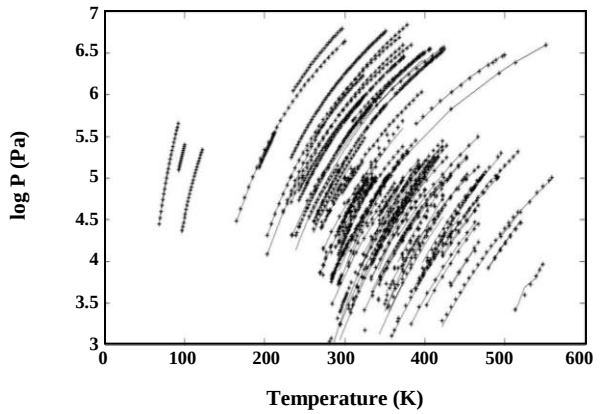

Fig. 5: Comparison between Patel-Teja predicted (-) and experimental data.

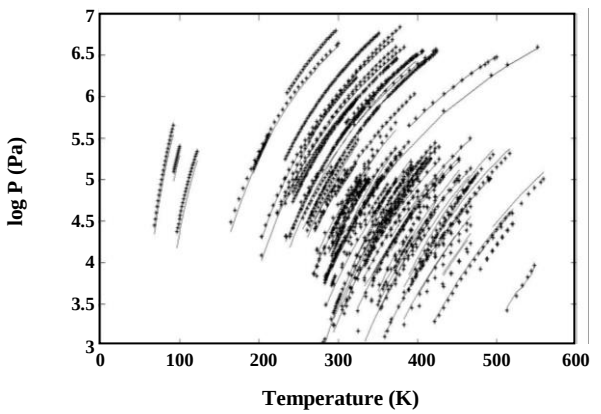

Fig. 6: Comparison between SRK predicted (-) and experimental data.

Appendix A

Instructions for running the program: The usage of the network is easy. Put the mat file (‘ANN_GCM.mat’) into the current folder of the MATLAB software (any version). Then, load the net to the workspace (using this command: _load (‘ANN_GCM.mat’). To get the value of vapor pressure from the net, you must follow the following example step by step:

Assume that you want to predict the vapor pressure of Ethyl butanoate at 360.7778 K. The group contribution parameters should be defined from the structure of Ethyl butanoate. The number of each group has been given in Table A.1.

Then following commands should be entered in the MATLAB command window:

>> input = [360.7778;567;3060;0.460990012;0;0;2;1;0;0;0;;1;0;1;0;0;0;0;0;0;0;0;0;0;0;0;0;0;0;0;0];

>> Preesure = sim(net,input)

Result is 39.4907, where its experimental value is equal to 33.4658 (ARD % is 0.0743).

Received : May 25, 2014 ; Accepted : Aug. 3, 2015

REFERENCES

[1] Gandhidasan P., Mohandes M.A., Predictions of Vapor Pressures of Aqueous Desiccants for Cooling Applications by Using Artificial Neural Networks, *Appl. Therm. Eng.*, **28**: 126-135 (2008).

[2] Peng D.Y., Robinson D.B., A New Two-Constant Equation of State, *Ind. Eng. Chem. Fundamen.*, **15**: 59-64 (1976).

[3] Soave G., Equilibrium Constants from a Modified Redlich–Kwong Equation of State, *Chem. Eng. Sci.*, **27**: 1197-1203 (1972).

[4] Patel N.C., Teja A.S., A New Cubic Equation of State for Fluids and Fluid Mixtures, *Chem. Eng. Sci.*, **37**: 463-473 (1982).

[5] Tu C.H., Group-contribution Method for the Estimation of Vapor Pressures, *Fluid Phase Equilib.*, **99**: 105-120 (1994).

[6] Avaullee L., Trassy L., Neau E., Jaubert J.N., Thermodynamic Modeling for Petroleum Fluids I. Equation of State and Group Contribution for the Estimation of Thermodynamic Parameters of Heavy Hydrocarbons, *Fluid Phase Equilib.*, **139**: 155-170 (1997).

[7] Marrero J., Gani R., Group-Contribution Based Estimation of Pure Component Properties, *Fluid Phase Equilib.*, **183**: 183-208 (2001).

[8] Coutsikos P., Voutsas E., Magoulas K., Tassios D.P., Prediction of Vapor Pressures of Solid Organic Compounds with a Group-Contribution Method, *Fluid Phase Equilib.*, **207**: 263-281 (2003).

[9] Moller B., Rarey J., Ramjugernath D., Estimation of the Vapour Pressure of Non-electrolyte Organic Compounds via Group Contributions and Group Interactions, *J. Mol. Liq.*, **143**: 52-63 (2008).

[10] Nannoolal Y., Rarey J., Ramjugernath D., Estimation of Pure Component Properties, Part 3. Estimation of the Vapor Pressure of Non-Electrolyte Organic Compounds via Group Contributions and Group Interactions, *Fluid Phase Equilib.*, **269**: 117-133 (2008).

[11] Ceriani R., Gani R., Liu Y.A., Prediction of Vapor Pressure and Heats of Vaporization of Edible Oil/Fat Compounds by Group Contribution, *Fluid Phase Equilib.*, **337**: 53-59 (2013).

[12] Ehsani M., Bateni H., Razi Parchikolaei G., Modeling of Oxidative Coupling of Methane over Mn/Na2WO4/ SiO2 Catalyst Using Artificial Neural Network, *Iran. J. Chem. Chem. Eng. (IJCCE)*, **32**(3): 107-114 (2013).

[13] Ahadian S., Moradian S., Mohseni, M. Determination of Surface Tension and Viscosity of Liquids by the Aid of the Capillary Rise Procedure Using Artificial Neural Network (ANN), *Iran. J. Chem. Chem. Eng. (IJCCE)*, **27**(1): 7-15 (2008).

[14] Potukuchi S., Wexler A.S., Predicting Vapor Pressures of Volatile Inorganic Components using Neural Networks, "14th Nucleation and Atmospheric Aerosols", p. 651 (1996).

[15] Kuhne R., Ebert R.U., Schtrmann G., Estimation of Vapour Pressures for Hydrocarbons and Halogenated Hydrocarbons from Chemical Structure by a Neural Network, *Chemosphere*, **34**: 671-686 (1997).

[16] Potukuchi W., Wexler A.S., Predicting Vapor Pressure using Neural Networks, *Atmos. Environ.*, **31**: 741-753 (1997).

[17] Lazzus J.A., Prediction of Solid Vapor Pressures for Organic and Inorganic Compounds Using a Neural Network, *Thermochim. Acta*., **489**: 53-62 (2009).

[18] Lazzus J.A., Estimation of Solid Vapor Pressures of Pure Compounds at Different Temperatures using a Multilayer Network with Particle Swarm Algorithm, *Fluid Phase Equilib.*, **289**: 176-184 (2010).

[19] Lazzus J.A., ρ–T–P Prediction for Ionic Liquids Using Neural Networks, *J. Taiwan Inst. Chem. E.*, **40**: 213-232 (2009).

[20] Rohani A.A., Pazuki G., Najafabadi H.A., Seyfi S., Vossoughi M., Comparison between the Artificial Neural Network System and SAFT Equation in Obtaining Vapor Pressure and Liquid Density of Pure Alcohols, *Expert Syst. Appl.*, **38**: 1738-1747 (2011).

[21] Moosavi M., Soltani N., Prediction of Hydrocarbon Densities Using an Artificial Neural Network-Group Contribution Method up to High Temperatures and Pressures, *Thermochim. Acta*, **556**: 89-96 (2013).

[22] Laugier S., Richon D., Use of Artificial Neural Networks for Calculating Derived Thermodynamic Quantities from Volumetric Property Data, *Fluid Phase Equilib.*, **210**: 247-255 (2003).

[23] Iliuta M.C., Iliuta I., Larachi F., Vapour-Liquid Equilibrium Data Analysis for Mixed Solvent-Electrolyte Systems Using Neural Network Models, *Chem. Eng. Sci.*, **55**: 2813-2825 (2000).

[24] Miyamoto H., Takemura J., Uematsu M., Vapour Pressures of Isobutane at T=(310 to 407) K, *J. Chem. Thermodyn.*, **36**: 919-923 (2004).

[25] Miyamoto H., Uematsu M., Measurements of Vapour Pressures and Saturated-Liquid Densities for n-Butane at T = (280 to 424) K, *J. Chem. Thermodyn.*, **39**: 827-832 (2007).

[26] Ewing M.B., Sanchez Ochoa J.C., The Vapour Pressures of n-Octane Determined Using Comparative Ebulliometry, *Fluid Phase Equilib.*, **210**: 277-285 (2003).

[27] N'Guimbi J., Berro C., Mokbel I., Rauzy E., Jose J., Experimental Vapour Pressures of 13 Secondary and Tertiary Alcohols-Correlation and Prediction by a Group Contribution Method, *Fluid Phase Equilib.*, **162**: 143-158 (1999).

[28] Censky M., Rohac V., Ruzicka K., Fulem M., Aim K., Vapor Pressure of Selected Aliphatic Alcohols by Ebulliometry. Part 1, *Fluid Phase Equilib.*, **298**: 192-198 (2010).

[29] Vecchio S., Brunetti B., Vapor Pressures and Standard Molar Enthalpies, Entropies, and Gibbs Free Energies of Sublimation of 2,4- and 3,4-Dinitrobenzoic Acids, *J. Chem. Thermodyn.*, **41**: 880-887 (2009).

[30] Falleiro R.M.M., Silva L.Y.A., Meirelles A.J.A., Krähenbühl M.A., Vapor Pressure Data for Fatty Acids Obtained using an Adaptation of the DSC Technique, *Thermochim. Acta*, **547**: 6-12 (2012).

[31] Cervantes M.C., Mokbel I., Champion D., Jose J., Voilley, A. Saturated Vapour Pressure of Aaroma Compounds at Various Temperatures, *Food Chem.*, **85**: 221-229 (2004).

[32] Shi L., Duan Y.Y., Zhu M.S., Han L.Z., Lei X., Vapor Pressure of 1,1,1,2,3,3,3-Heptafluoropropane, *Fluid Phase Equilib.*, **163**: 109-117 (1999).

[33] Stull D.R., Vapor Pressure of Pure Substances Organic and Inorganic Compounds, *Ind. Eng. Chem.*, **39**: 517-540 (1947).

[34] A.H.N. Mousa, Vapour Pressure and Saturated-Vapour Volume of Acetonitrile, *J. Chem. Thermodyn.*, **13**: 201-202 (1981).

[35] Felsing W.A., Durban S.A., The Vapor Pressure, Densities, and Some Derived Quantities for Acetone, *J. Am. Chem. Soc.*, **48**: 2885-2893 (1926).

[36] Ambrose D., Hall D.J., Thermodynamic Properties of Organic Oxygen Compounds L. The Vapour Pressures of 1,2-ethanediol (Ethylene Glycol) and bis(2-hydroxyethyl) ether (diethylene glycol), *J. Chem. Thermodyn.*, **13**: 61-66 (1981).

[37] Taylor R.S., Smith L.B., The Vapor Pressures, Densities and some Derived Quantities for Ether at Low Temperatures, *J. Am. Chem. Soc.*, **44**: 2450-2463 (1922).

[38] . Eon C, Pommier C., Guiochon G., Vapor Pressures and Second Virial Coefficients of Some Five-Membered Heterocyclic Derivatives, *J. Chem. Eng. Data*, **16**: 408-410 (1971).

[39] Ambrose D., Townsend R., Thermodynamic Properties of Organic Oxygen Compounds. Part IX. The Critical Properties and Vapour Pressures, above Five Atmospheres, of Six Aliphatic Alcohols, *J. Chem. Soc.* **54**: 3614-3625 (1963).

[40] Philippe R., Jambon C., Cléchet P., Thermodynamic Properties of Dimethylsulfoxide + Halomethane Mixtures II. Vapour Pressures and Excess Thermodynamic Functions, *J. Chem. Thermodyn.*, **5**: 431-444 (1973).

[41] Li I.P.C., Lu B.C.Y., Chen E.C., Vapor-Liquid Equilibriums of Binary Systems Containing n-hexane, Cyclohexane, and Benzene at Low Temperatures, *J. Chem. Eng. Data*, **18**: 305-309 (1973).

[42] Plesnar Z., Fu Y.H., Sandler S.I., Orbey H., Vapor-Liquid Equilibrium of the Acetic Acid + Octane Binary System at 323.15 K and 343.15 K, *J. Chem. Eng. Data*, **41**: 799-801 (1996).

[43] Carruth G.F., Kobayashi R., Vapor Pressure of Normal Paraffins Ethane Through n-decane from Their Triple Points to About 10 mm Hg, *J. Chem. Eng. Data*, **18**: 115-126 (1973).

[44] Daubert T.E., Jalowka J.W., Goren V., Vapor Pressure of 22 Pure Industrial Chemicals, *AIChE Symp. Ser.*, **83**: 128-156 (1987).

[45] Dejoz A., Alfaro V.G., Miguel P.J., Vázquez M.I., Isobaric Vapor-Liquid Equilibria of Tetrachloroethylene + 1-propanol and + 2-propanol at 20 and 100 kPa, *J. Chem. Eng. Data*, **41**: 1361-1365 (1996).

[46] Dever D.F., Finch A., Grunwald E., The Vapor Pressure of Methanol, *J. Phys. Chem.*, **59**: 668-669 (1955).

[47] Gibbard H.F., Creek J.L., Vapor Pressure of Methanol from 288.15 to 337.65 K, *J. Chem. Eng. Data*, **19**: 308-310 (1974).

[48] Fowler L., Trump W.N., Vogler C.E., Vapor Pressure of Naphthalene. Measurements between 40 deg and 180 deg, *J. Chem. Eng. Data*, **13**: 209-210 (1968).

[49] Pividal K.A., Sterner C., Sandler S.I., Orbey H., Vapor-Liquid Equilibrium from Infinite Dilution Activity Coefficients: Measurement and Prediction of Oxygenated Fuel Additives with Alkanes, *Fluid Phase Equilib.*, **72**: 227-249 (1992).

[50] Rintelen J.C., Saylor J.H., Gross P.M., The Densities and Vapor Pressures of some Alkylbenzenes, Aliphatic Ketones and n-Amyl Chloride, *J. Am. Chem. Soc.*, **59**: 1129-1130 (1937).

[51] Kassel L.S., Vapor Pressures of the Xylenes and Mesitylene, *J. Am. Chem. Soc.*, **58**: 670-671 (1936).

[52] Camin D.L., Forziati A.F., Rossini F.D., Physical Properties of n-Hexadecane, n-Decylcyclopentane, n-Decylcyclohexane, 1-Hexadecene and n-Decylbenzene, *J. Phys. Chem.*, **58**: 440-442 (1954).

[53] Lee F.M., Coombs D.M., Two-Liquid-Phase Extractive Distillation for Aromatics Recovery, *Ind. Eng. Chem. Res.*, **26**: 564-573 (1987).

[54] Bryson C.E., Cazcarra V., Levenson L.L., Sublimation Rates and Vapor Pressures of H_2O, CO_2, N_2O, and Xe, *J. Chem. Eng. Data*, **19**: 107-110 (1974).

[55] Kleinrahm R., Duschek W., Wagner W., (Pressure, Density, Temperature) Measurements in the Critical Region of Methane, *J. Chem. Thermodyn.*, **18**: 1103-1114 (1986).

[56] Wagner W., New Vapour Pressure Measurements for Argon and Nitrogen and a New Method for Establishing Rational Vapour Pressure Equations, *Cryogenics*, **13**: 470-482 (1973).

[57] Barnett F.D., Harvey N.D., Vapor Pressure of Liquid Oxygen and Nitrogen, *J. Am. Chem. Soc.*, **49**: 610-620 (1927).

[58] Razzouk A., Hajjaji A., Mokbel I., Mougin P., Jose J., Experimental Vapor Pressures of 1,2-bis(dimethylamino)ethane, 1-methylmorpholine, 1,2-bis(2-aminoethoxy)ethane and N-benzylethanolamine between 273.18 and 364.97K, *Fluid Phase Equilib.*, **282**: 11-13 (2009).

[59] Bejarano A., Poveda L.J., de la Fuente J.C., Supplementary Vapor Pressure Data of the Glycol Ethers, 1-methoxy-2-propanol, and 2-methoxyethanol at a Pressure Range of (15 to 177) kPa, *J. Chem. Thermodyn.*, **53**: 114-118 (2012).

[60] Bejarano A., Quezada N., de la Fuente J.C., Complementary Vapor Pressure Data for 2-methyl-1-propanol and 3-methyl-1-butanol at a Pressure Range of (15 to 177) kPa, *J. Chem. Thermodyn.*, **41**: 1020-1024 (2009).

[61] Mokbel I., Rauzy E., Loiseleur H., Berro C., Jose j., Vapor Pressures of 12 Alkylcyclohexanes, Cyclopentane, Butylcyclopentane and Trans-Decahydronaphthalene Down to 0.5 Pa. Experimental Results, Correlation and Prediction by an Equation of State, *Fluid Phase Equilib.*, **108**: 103-120 (1995).

[62] Gregorowicz J., Kiciak K., Malanowski S., Vapour Pressure Data for 1-butanol, Cumene, n-octane and n-decane and Their Statistically Consistent Reduction with the Antoine Equation, *Fluid Phase Equilib.*, **38**: 97-107 (1987).

[63] Rohac V., Ruzicka K., Ruzicka V., Zaitsau D.H., Kabo G.J., Diky V., Aim K., Vapour Pressure of Diethyl Phthalate, *J. Chem. Thermodyn.*, **36**: 929-937 (2004).

[64] Sawaya T., Mokbel I., Rauzy E., Saab J., Berro C., Jose J., Experimental Vapor Pressures of Alkyl and Aryl Sulfides Prediction by a Group Contribution Method, *Fluid Phase Equilib.*, **226**: 283-288 (2004).

[65] Fu Y., Han L., Zhu M.S., PVT Properties, PVT Properties, Vapor Pressures and Critical Parameters of HFC-32, *Fluid Phase Equilib.*, **111**: 273-286 (1995).

[66] Cui X., Chen G., Han X., Wang Q., Experimental Vapor Pressure Data and a Vapor Pressure Equation for Fuoroethane (HFC-161), *Fluid Phase Equilib.*, **245**: 155-157 (2006).

[67] Feng X., Xu X., Lin H., Duan Y., Vapor Pressures of 1,1,1,2,3,3,3-heptafluoropropane, 1,1,1,3,3,3-hexafluoropropane and 1,1,1,3,3-pentafluoropropane, *Fluid Phase Equilib.*, **290**: 127-136 (2010).

[68] Ambrose, D. Ellender J.H., Lees E.B., Sprake C.H.S., Townsend R., Thermodynamic Properties of Organic Oxygen Compounds XXXVIII. Vapour Pressures of Some Aliphatic Ketones, *J. Chem. Thermodyn.*, 7: 453-472 (1975).

[69] Weber L.A., Ebulliometric Measurement of the Vapor Pressures of R123 and R141b, *Fluid Phase Equilib.*, **80**: 141-143 (1992).

[70] Farkova J., Wichterle I., Vapour Pressures of Some Ethyl and Propyl Esters of Fatty Acids, *Fluid Phase Equilib.*, **90**: 143-148 (1993).

[71] Straty G.C., Tsumura R., PVT and Vapor Pressure Measurements on Ethane, *J. Res. Nbs. A Phys. Ch.*, **80**: 35-39 (1976).

[72] Duan Y.Y., Zhu M.S., Han L.Z., Experimental Vapor Pressure Data and a Vapor Pressure Equation for Trifluoroiodomethane (CF3I), *Fluid Phase Equilib.*, **121**: 227-234 (1996).

[73] Reid R.C., Prausnitz J.M., Poling B.E., "The Properties of Gases and Liquids", 4th ed., McGraw-Hill Book Company, New York (1987).

[74] Perry, D. Green (Eds.), "Perry's Chemical Engineers Handbook", 7th Edition, McGraw-Hill, New York (1997).

[75] The Dortmund Data Bank, http://www.ddbst.com/.